Ethanol gas sensing properties of nano-porous $LaFeO_3$ thick films

S.M.Khetre[*a], A.U.Chopade[a], C.J.Khilare[a], S.R.Kulal[b] H.V.Jadhav[c], P.N.Jagadale[c], S.V.Bangale[c], , S.R.Bamane[c]

[a]*Dahiwadi College Dahiwadi, Tal.Man, Dist. Satara, (M.S.) 415508 India*

[b]*Devchand College Arjunnagar, Kolhapur*

[c]*Metal Oxide Research Laboratory, Dr.Patangrao Kadam Mahavidhyalaya Sangli.*

Email- sanjaykhetre@gmail.com Tel. +91-2165-220231 Fax.+ 91-2165-220231

Abstract.

The characterization and ethanol gas sensing properties of nanoporous $LaFeO_3$ thick films were studied. Thick films of nanoporous $LaFeO_3$ were observed to be highly sensitive to ethanol vapours at 300 °C. Upon exposure of ethanol vapours, the barrier height would decrease greatly leading to drastic increase in conductance. It is reported that the surface misfits and operating temperature can affect the microstructure and gas sensing performance of the sensor. The quick response and fast recovery are the main features of this sensor. The effects of microstructure and additive concentration on the gas response, selectivity, response time and recovery time of the sensor in the presence of ethanol vapours were studied.

Keywords: Nanoporous $LaFeO_3$; Gas response.

1. Introduction:

Environmental safety is one of the serious concerns for the scientific community because of rapid increase in the use of organic pollutants in agriculture and various industries which caused severe adverse effects on the environment. Among various organic pollutants, ethanol, a colorless liquid, is one of the pollutants which is widely used as an industrial solvent for the preparation of various materials. [1-2] It easily mixed with water and hence causes oxidative damage of brain, stomach, liver, erythrocyte, etc. [3-4] Due to its high-toxic nature, it is highly needed to detect efficiently the presence of ethanol in the environment.

In this work, a successful synthesis of $LaFeO_3$ nano sheet via combustion process was done and characterized in terms of their structural and optical properties. Importantly, as-synthesized $LaFeO_3$ nanosheets were efficiently utilized as redox mediator for the fabrication of efficient ethanol chemi-sensor which exhibits good sensor performance, specifically in terms of its sensitivity and detection limit.

2. Experimental

Analytical grade $La(NO_3)_3 \cdot 6H_2O$, $Fe(NO_3)_3 \cdot 9H_2O$ and $C_2H_5NO_2$ were used as raw materials to prepare $LaFeO_3$. According to the stoichiometric preparation of the reactants, the specified amounts of $Fe(NO_3)_3 \cdot 9H_2O$ and $La(NO_3)_3 \cdot 6H_2O$ were first dissolved in glycine solution to form the sol. The molar amount of glycine was double to total molar amount of metal nitrates in the solution. A small amount of ammonia aqueous was slowly added to adjust the pH to 7. During this procedure, the solution was continuously stirred and kept at a temperature of 60-70 ^{0}C. Then, the stabilized nitrate–glycine sol was poured into a tray and heated slowly to 140-150 ^{0}C.Viscosity and color changed as the sol turned into a green, puffy, porous dry gel. The entire combustion process would last a few seconds. The as-synthesis powder was the nanocrystalline $LaFeO_3$ with fine crystal structure.

2.1. Thick film preparation

The thixotropic paste was screen printed on a glass substrate in desired patterns. [5] The films prepared were fired at 550^{0}C for 24 h. These films were surface modified by dipping them into a 0.01M aqueous solution of cupric chloride for different intervals of time and were dried at 80^{0}C followed by firing at 550^{0}C for 24 h in air ambient. The $CuCl_2$ dispersed on the films was oxidized in firing process, and sensor elements with different mass% of $LaFeO_3$ were obtained. Silver contacts were made by vacuum evaporation for electrical measurements. [6]

3.Results and discussion

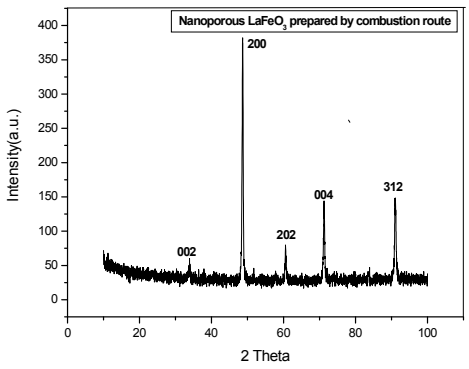

Fig.1 XRD of $LaFeO_3$ nanoporous material

3.1. XRD analysis:

The XRD measurement (Fig. 1) shows that the product is pure perovskite oxide $LaFeO_3$ with an orthorhombic structure, the diffraction data are in good agreement with JCPDS card of $LaFeO_3$ (JCPDS no: 15-0148). The average crystalline size of $LaFeO_3$ perovskite powder is determine with the help of Scherrer's equation $t=0.9\lambda/\beta cos\theta$, where t is the average size of the particles, λ is wavelength of X-ray

radiation, β the full width at half maximum of the diffracted peak and θ is the angle of diffraction .[7-10] The average crystalline size obtained for nanocrystalline $LaFeO_3$ calcinated at 1000 ^{0}C is found to be 28-63 nm. Fuel plays an important role in the combustion of gel. At the combustion point organic fuel formed H_2O , CO_2, N_2 gases and they tried to come out from the gel by breaking the gel into nanoporous and nanosized particles of $LaFeO_3$.

3.2. SEM analysis:

The SEM technique was employed for finding morphology of $LaFeO_3$ powder heated at 1000 ^{0}C. [Fig. 2] One can notice the presence of macro-agglomerations of very fine particles having size less than 1μm. The particle shapes are not well defined. Many large and small pores are present in the whole material. We assumed that the pores are mainly intergranular because intragranular pores are not seen on the SEM photograph.

3.3.TEM analysis:

The TEM specimens were prepared by placing microdrops of colloid solutions on a carbon film supported by a copper grid.

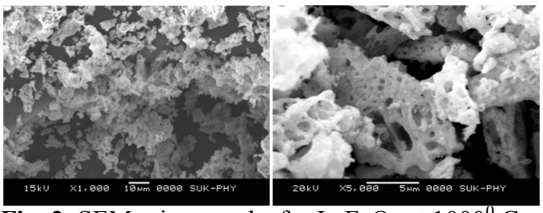

Fig. 2 SEM micrographs for $LaFeO_3$ at 1000^0 C

The TEM images of the nanocrystalline $LaFeO_3$ calcinated at 1000 ^{0}C in air for 5 h are shown in [Fig. 3 (a)] it indicates the presence of $LaFeO_3$ nanoparticles with 28-63 nm size which form spherical type of oriental aggregation, agglomeration and polymeric linkage throughout the region.

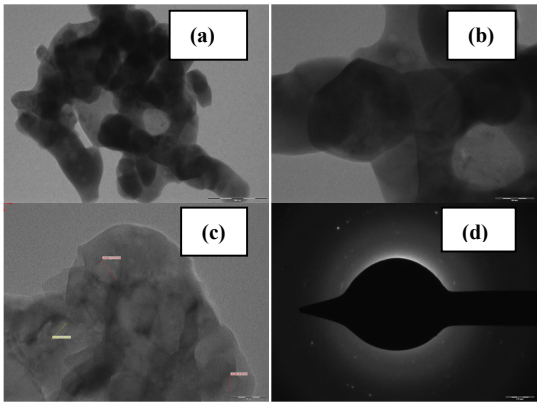

Fig. 3 TEM image of $LaFeO_3$ calcinated at 1000 ^{0}C (a): high resolution transmission electron microscopy image of nanocrystalline $LaFeO_3$ (b-c): selected area electron diffraction pattern (d).

The HRTEM image [Fig. 3 (b-c)] shows the porous nature of the material. The pores are well developed spherical shape with diameter from 9-13 nm size. The results are correlated with the XRD.The selected area diffraction (SAED) pattern [Fig 4 (d)] shows the spot type pattern which is indicative of single crystalline particles. No evidence was found for more than one pattern, suggesting the single phase nature of the material. The surface area of the synthesized powder is 15.5 m^2/g.

4. Electrical Properties

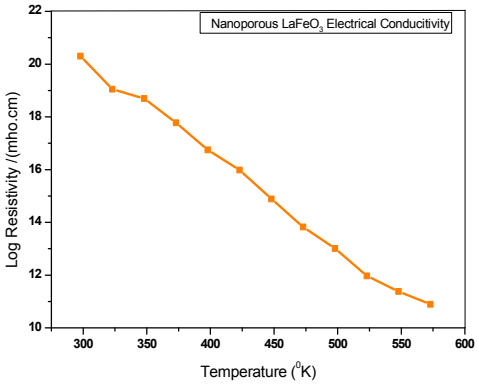

Fig.4. Conductance-temperature profiles of $LaFeO_3$ sample in air.

4.1 Electrical conductivity

The semiconducting nature of $LaFeO_3$ is observed from the measurements of resistivity with temperature. The semiconductivity in $LaFeO_3$ must be due to large oxygen deficiency in it. The material would then adsorb the oxygen species at higher temperatures ($O_2^- \rightarrow 2O^- \rightarrow O^{2-}$). The increase in conductivity with increasing temperature could be attributed to negative temperature coefficient of resistance and semiconducting nature of the $LaFeO_3$. It is observed from [Fig.4] that the electrical conductivity of the $LaFeO_3$ is nearly linear in the temperature range from 300–575°K in air ambient.

5. Sensing Performance

5.1. Gas response and operating temperature

It is clear from the [Fig.5] that the gas response increase with operating temperature reaches to the maximum (100 ppm) at 300 ^{0}C, and falls with further increasing the in operating temperature. The ethanol may burn before reaching the surface of the film at higher temperatures (>300 ^{0}C). Hence, the gas response would have been decreased above 300 ^{0}C.A larger amount of oxygen-adsorption would have occurred on the surface of the film at 300 ^{0}C and have facilitated the sensor to oxidize the ethanol gas immediately, giving faster and larger gas response.

5.2. Selectivity for ethanol against various gases

Fig. 6 depicts the selectivity of $LaFeO_3$ to 100 ppm of ethqnol gas against various gases at 300 ^{0}C. It is clear from Fig. 6 that, in contrast to pure $LaFeO_3$; the sample shows not only enhanced response towards ethanol but also very high selectivity.

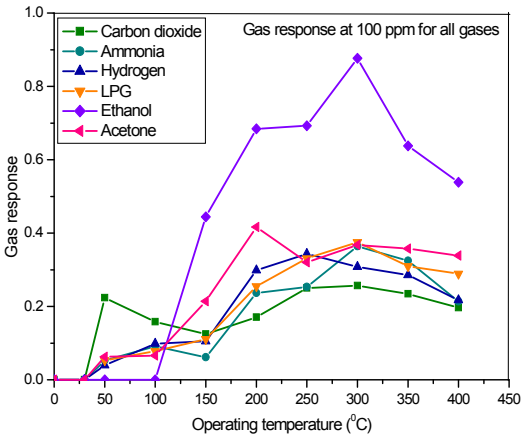

Fig. 5. Variation of gas response with operating temperature.

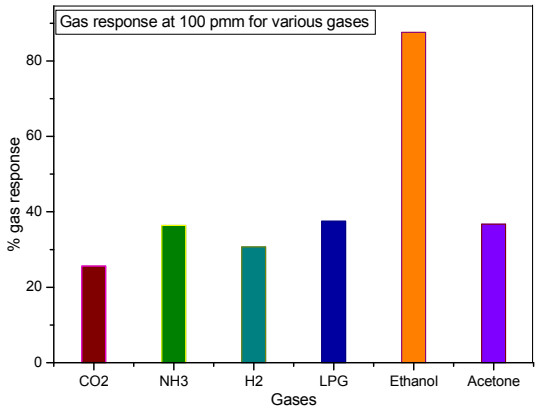

Fig.6 Gas responses among various gases

5.3. Response and recovery of the sensor

The response and recovery of the $LaFeO_3$ sensor are represented in Fig. 7. The response was quick (≈5 s) to 100 ppm of ethanol. Recovery was also very fast (≈35s). The fast response may be due to the fast oxidation of ethanol into H_2O (gas). After sevaporating water molecules, the film recovery was obtained.

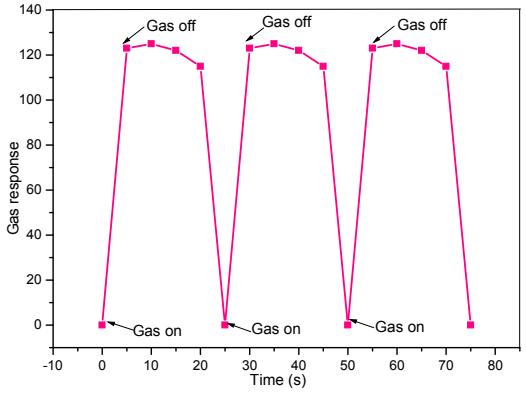

Fig.7 The gas response and recovery of the $LaFeO_3$ sensor

6. Conclusion

(1)Pure $LaFeO_3$ nanoporous material was successfully synthesized by combustion method.

(2) Nanoporous $LaFeO_3$ was characterized by XRD, SEM,TEM techniques.

(3) Nanoporous $LaFeO_3$ showed good electrical conductivity .

(4) The optimum operating temperature for ethanol gas sensing was 300 ^{0}C.

(5) $LaFeO_3$ has the potential of fabricating ethanol sensor.

(6) The $LaFeO_3$ thick film sensor showed very rapid response and recovery to ethanol gas.

(7) The sensor showed good selectivity to ethanol gas against LPG, NH_3, CO_2, Acetone, CO_2 and H_2 gases.

References

[1] G. X.. Zheng , J. M. Song, Y. H. Wang , S. P. Yu, Huan Jing Ke Xue 30, (2009), 1306–14.

[2] L. Senf, F Stapf, B .Düsedau, H . Frank. J Therm Anal Calorim 33 , (1988) , 371–4.

[3] S C Bondy, S.X. Guo. Eur J Pharmacol 270, (1994), 349–55.

[4] C . Lindi, G .Montorfano, P. Marciani. Alcohol 16, (1998), 311–6.

[5] Z .Tianshua, P .Hinga, Z .Jiancheng, K. Lingbing. Mater Chem Phys , 61 , (1999), 192–8.

[6] Y .Mu, J . Yang, S . Han, H .Hou, Y . Fan. Mater Lett , 64, (2010), 1287–90.

[7] S. M. Khetre, H. V. Jadhav , P. N. Jagadale, S. R. Kulal , S. R. Bamane, Advances in Applied Science Research, 2 (4), (2011), 503-511

[8] S. M. Khetre, C. J. Khilare, V. S Shivankar, S. R. Bamane , Sensors & Transducers Journal, 137(2) (2012), 165-175

[9] S. R.Kulal , S.M..Khetre ,P.N. Jagdale, V. M. Gurame , D.P.Waghmode, G.B. .Kolekar , S.R. Sable, S.R.Bamane , Materials Letters 84, (2012), 169–172

[10] S. M. Khetre, H. V. Jadhav, S. R. Bamane, Rasayan Journal of Chemistry, 2(1) (2009), 174-178